SINGLE WALL CARBON NANOTUBE FIBERS EXTRUDED FROM SUPER-ACID SUSPENSIONS: PREFERRED ORIENTATION, ELECTRICAL AND THERMAL TRANSPORT

W. Zhou[1], J. Vavro[1], C. Guthy[1], K. I. Winey[1], J. E. Fischer[1], L. M. Ericson[2], S. Ramesh[2], R. Saini[2], V. A. Davis[2], C. Kittrell[2], M. Pasquali[2], R. H. Hauge[2] and R. E. Smalley[2]

[1]Department of Materials Science and Engineering
University of Pennsylvania, Philadelphia PA 19104-6272
[2]Center for Nanoscale Science and Technology
Rice University, Houston TX 77005

Corresponding author e-mail address: fischer@seas.upenn.edu

Introduction

Macroscopic oriented arrays of single wall carbon nanotubes (SWNT) [1-4] are far more attractive for practical applications than the random tangles of bundled tubes typically found in as-grown bulk samples. In fiber form, such arrays could be the starting point for the construction of useful structures which largely maintain the excellent axial properties expected from atomically perfect SWNT. Such fibers produced by the HiPco process [5] offer promise for high strength, light weight, thermally and electrically conducting structural elements at lower cost than other nanotube forms.

Fibers extruded from super-acid suspensions of HiPco SWNT exhibit preferred orientation along their axes. We characterize the alignment by x-ray fiber diagrams and polarized Raman scattering. Alignment, electrical and thermal transport all improve with decreasing extrusion orifice diameter. Resistivity ρ, thermoelectric power [6] and resonant-enhanced Raman scattering [7] indicate that the neat fibers are strongly p-doped. The lowest observed ρ is 0.25mΩcm at 300 K. High temperature annealing *increases* ρ by more than an order of magnitude.

Experimental

The fibers are poorly crystalline so we analyze the diffuse x-ray scattering from weakly correlated SWNT to describe the degree of orientation by a mosaic full width at half-maximum (FWHM). This is obtained from the azimuthal dependence of diffuse intensity summed over an appropriate Q range using pinhole optics and a 2-D detector [7]. The data indicate that some fraction of the nanotubes are aligned while the rest

remain randomly oriented, suggesting poorly-dispersed aggregates, short tubes which don't orient well when extruded through a large needle, etc. The FWHM of the orientation distribution function is accurately and unambiguously obtained from x-ray data, and ranges from 44° to 64° under different extrusion conditions. Combined with angle-dependent polarized Raman spectra [4,7,8], we also get a good estimate for the aligned fraction, generally greater than 80% and again dependent on extrusion conditions.

Fibers were made by suspending purified HiPco SWNT [5] in oleum (>100% H_2SO_4), then extruding into an ether coagulation bath using a syringe pump [9]. Sample HPR93A was extruded from 8 wt.% SWNT through a 500 μm needle; HPR93B was extruded from 6 wt.% through a 125 μm needle, and HPR93C was extruded from 6 wt.% SWNT through a 250 μm needle. No mechanical stretching was applied after extrusion [10]. Properties were measured before and after vacuum annealing at 1100°C for 24 hours. Polarized Raman measurements were done in VV geometry on a Renishaw Ramanscope 1000 using 514.4 nm excitation and 2 μm diameter spot size. Resistivity was measured by a four-probe DC technique. Voltage probes were about 2-3 mm apart. Thermal conductivity κ was measured from 10 to 300 K using a comparative technique [4,7]. The accuracy of ρ and κ data, estimated as $\pm$ 30%, is limited by errors in cross-sectional area. Sample densities were not determined so no corrections for porosity were made.

Results and Discussion

We present a sampling of the data and then summarize in tabular form. Figure 1 shows the azimuthal dependence of x-ray intensity corresponding to the first-order Bragg peak of the 2-D triangular lattice of SWNT ordered into "ropes" [11]. For this fiber the Gaussian FWHM is 55^{o} before and after annealing.

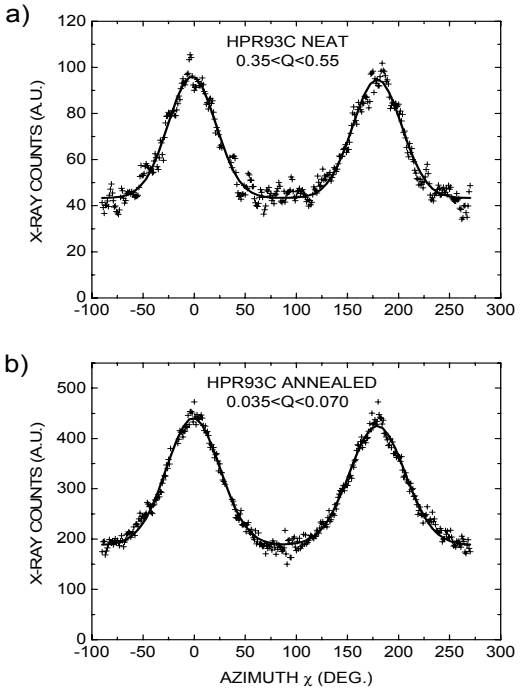

Figure 1. Circumferential intensity plot From a 2-D x-ray fiber diagram; the Bragg angle corresponds to the (1,0) reflection of a 2-D triangular lattice with **a** = 14.2 Å. Data shown a) before and b) after annealing, for the 6 wt%/250 μm sample.

All 3 fibers exhibit low resistance before annealing, with metallic temperature dependence $d\rho/dT > 0$ above 200 K (Figure 2 left panel). For the best-aligned HPR93B, ρ(300 K) = 0.24 mΩcm, only a factor 10 greater than graphite in-plane. For all 3 fibers, both the small values and the weak temperature dependence are due to the strong redox doping effect of bisulfate from the acid suspension [12]. Thermopower measurements on neat fibers suggest that the Fermi level is shifted by 0.55 eV into the valence band [6] so that the semiconducting tubes are degenerately p-doped and thus contribute to electrical conductivity. We also suspect that doping strongly "improves" the interparticle (e.g. rope-rope) contacts, suppressing the low T upturn in resistivity. Similar behavior is observed in alkali-doped buckypaper samples [13].

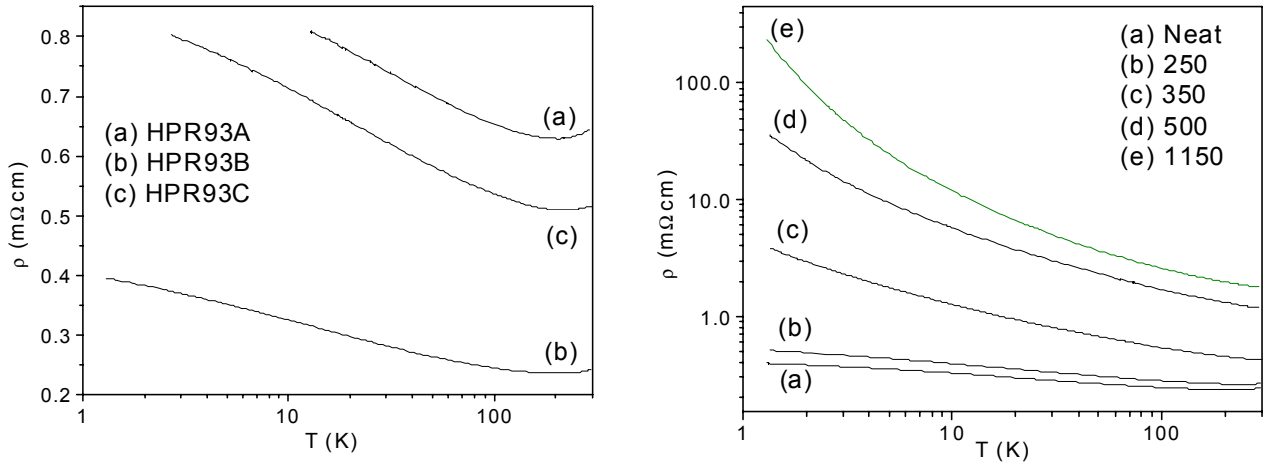

Figure 2. (left) ρ vs. T for the 3 neat fibers. ρ decreases at all T as alignment improves (see table). Non-metallic behavior at low T levels off as $T \rightarrow 0$, while metallic behavior is observed above 200K. (right) Effect of vacuum annealing on ρ(T) for HPR93B; note log-log scale. ρ increases as the bisulfate p-dopants are removed, especially at low T.

The effect of annealing on resistivity is shown in the right panel of Figure 2. HPR93B was annealed for 15 min. at successively higher temperatures. Annealing removes the p-dopant bisulfate ions which arise from residues of the oleum solvent when the fibers are exposed to air. Thus they become more resistive with higher annealing temperatures. The first annealing temperature has little effect, while there is a notable change after the 350^{o}C anneal. This suggest that bisulfate anions are incorporated into the bundles and desorb with an activation energy ~ 250-350 k_BT. Neat and annealed values of ρ(300 K) are included in Table I. Note that ρ vs. T differs greatly from that of the neat fibers. All 3 annealed samples show large increases in ρ at all T, in addition to notably steeper non-metallic temperature dependence. These results suggest that de-doping leads to localization of charge carriers within the ropes. Another possibility is that annealing changes some property of interparticle contacts such that carriers can now be trapped there as well.

The totality of results are summarized in Table I. The FWHM's decrease continuously with decreasing orifice diameter, but are unaffected by annealing. Aligned fractions $\mathcal{A}$ also improve with decreasing orifice diameter, and are also unaffected by annealing. It is gratifying that both annealed and unanealed resistivities *decrease* with increasing degree of alignment, the neat values being ~ 10 times lower due to acid doping (confirmed by p-type thermopower). Thermal conductivity shows a large initial improvement from sample A to B, but nothing significant as the orifice diameter is halved. This suggests that κ depends more strongly on SWNT concentration in the precursor suspension than on the alignment.

	HPR93A		HPR93C		HPR93B	
Concentration	8 wt.%		6 wt.%		6 wt.%	
Extrusion orifice diameter (μm)	500		250		125	
	Neat	Annealed	Neat	Annealed	Neat	Annealed
FWHM (deg.) (from x-ray)	63	64	55	54	45	43
$\mathcal{A}$ ($\pm$0.02) (from Raman)	0.83	0.86	0.90	0.92	0.94	0.95
ρ(300K)(mΩcm)	0.64	8.10	0.51	5.51	0.25	2.62
κ(300K)(W/mK)	5.0	5.0		19		17

Table I. Summary of the synthesis parameters, texture analysis fit parameters and room temperature electrical resistivities and thermal conductivities for neat and annealed HiPco fibers. FWHM is the Gaussian distribution width of SWNT axes with respect to the fiber axis, determined from x-ray scatteriong. A is the aligned fraction, determined from Raman using the FWHM from x-ray as an input.

Conclusions

The macroscopic alignment exhibited by SWNT fibers extruded from oleum probably results from a combination of local ordering in suspension (as observed from their birefringent and rheological behavior [9]) and flow-induced reorientation of these ordered domains during extrusion. Mechanical stretching after extrusion may reduce the FWHM even further [10]. Improvements in fiber alignment and properties would be facilitated by a more complete understanding of the nanotube suspensions [14].

Structural analysis combining x-ray and Raman scattering unambiguously shows that smaller orifice diameter generally results in fibers with better alignment. Compared to magnetic field-aligned films [4], anisotropic flow without mechanical shear results in larger aligned fractions and slightly broader distribution widths for the fibers. Resistivity and thermopower measurements show that the neat fibers are heavily p-doped. In general the correlation between resistivity and alignment is excellent. Annealing in

vacuum drives out the dopants, resulting in higher resistivity, non-metallic temperature dependence and restoration of resonant-enhanced Raman scattering [7]. Thermal conductivity is also improved by alignment; room temperature values range from 5 to 20 W/m-K for samples with the poorest and best FWHM and aligned fraction respectively.

Acknowledgments

This work is supported by ONR under the DURINT program, Grant No. N00014-01-1-0789. Shared facilities were provided by the Penn MRSEC program, Grant No. DMR00-79909.

References

[1] L. Jin. C. Bower and O. Zhou, Appl. Phys. Lett. **3**, 1197 (1998).
[2] J. C. Hone, M. C. Llaguno, N. M. Nemes, J. E. Fischer, D. E. Walters, M. J. Casavant, J. Schmidt and R. E. Smalley, Appl. Phys. Lett. **77**, 666 (2000).
[3] P. Launois, A. Marucci, B. Vigolo, A. Derre and P. Poulin, J. Nanoscience and Nanotechnology **1,** 1255 (2001); B. Vigolo, P. Poulin, M. Lucas, P. Launois and P. Bernier, Appl. Phys. Letters **81** 1210 (2002).
[4] J. E. Fischer, W. Zhou, J. Vavro, M. C. Llaguno, C. Guthy, R. Haggenmueller, K. I. Winey, M. J. Casavant and R. E. Smalley, J. Appl. Phys. **93,** 2157 (2003).
[5] I. W. Chiang, B. E. Brinson, A. Y. Huang, P. A. Willis, M. J. Bronikowski, J. L. Margrave, R. E. Smalley, and R. H. Hauge, J. Phys. Chem. B **105**, 8297 (2001).
[6] Vavro, M. C. Llaguno, J. E. Fischer, S. Ramesh, R. K. Saini, L. M. Ericson, V. A. Davis, M. Pasquali, R. E. Smalley, Phys. Rev. Lett. **90,** 065503 (2003).
[7] W. Zhou, J. Vavro, C. Guthy, K. I. Winey, J. E. Fischer, L. M. Ericson, S. Ramesh, R. K. Saini, V. A. Davis, C. Kittrell, M. Pasquali, R. H. Hauge and R. E. Smalley, *J. Appl. Physics* **95**, 649 (2004).
[8] H. H. Gommans, J. W. Alldredge, H. Tashiro, J. Park, J. Magnuson and A. G. Rinzler, J. Appl. Phys. **88**, (2000) 2509.
[9] V. A. Davis, L.M. Ericson, A. N. G. Parra-Vasquez, H. Fan, Y. Wang, V. Prieto, J. A. Longoria, J. A, S. Ramesh, R. K. Saini, C. Kittrell, W. E. Billups, W. W. Adams, R. H. Hauge, R. E. Smalley and M. Pasquali, M.; Macromolecules; **37,** 154 (2004).
[10] . B. Vigolo, A Penicaud, C. Coulon, C. Sauder, R. Pallier, C. Journet, P. Bernier and P. Poulin, Science **290,** 1331 (2000).
[11]. A. Thess, R. Lee, P. Nikolaev, H. Dai, P. Petit, J. Robert, C. Xu, H. Lee, S.G. Kim, D. T. Colbert, G. Scuseria, D. Tomanek, J. E. Fischer and R. E, Smalley, Science **273**, 483 (1996).
[12] A. Metrot and J.E. Fischer, Synthetic Metals **3**, 201 (1981).
[13] R. S. Lee, H. J. Kim, J. E. Fischer, J. Lefebvre, M. Radosavljević, J. Hone and A. T. Johnson, Phys. Rev. B **61**, 4526 (2000).
[14] W. Zhou, M. F. Islam, H. Wang, D. Ho, A. G. Yodh, K. I. Winey and J. E. Fischer, Chem. Physics Letters **384**, 185 (2004).